Timing of the last deglaciation phases in the southern Baltic area inferred from Bayesian age modeling

Karol Tylmann[1], Szymon Uścinowicz[2]

[1] Faculty of Oceanography and Geography, University of Gdańsk, Aleja Marszałka Piłsudskiego 46, 81-378 Gdynia, Poland
[2] Institute of Hydro-Engineering of Polish Academy of Sciences, Kościerska 7, 80-328 Gdańsk, Poland

Corresponding author: Karol Tylmann, e-mail: k.tylmann@ug.edu.pl

Non-peer reviewed preprint submitted to EarthArXiv

Submitted to *Quaternary Science Reviews* February 1, 2022

Highlights:

- New chronology of the last deglaciation phases in the southern Baltic basin
- Space-time correlation of ice marginal landforms across the southern Baltic
- Time-slice reconstruction of the southern Scandinavian Ice Sheet (18–14 ka)
- Retreat rate of the southern margin of the last ice sheet about 40–55 m/yr

Abstract

A new chronology of the last Scandinavian Ice Sheet retreat in the southern Baltic basin is proposed. Based on Bayesian age modeling, we show that the most likely ages of particular deglaciation phases are 16.5 ± 0.5 ka for the Gardno Phase, 15.6 ± 0.6 ka for the Słupsk Bank Phase, and 13.9 ± 0.5 ka for the Southern Middle Bank Phase. The Gardno moraines are correlated with the Halland Coastal moraines in southern Sweden and the Middle Lithuanian moraines in Lithuania and Latvia. Ice margin stillstands of the Słupsk Bank Phase and Souhern Middle Bank Phase are correlated with the Göteborg and Vimmerby moraines, and with the North Lithuanian (Haanja) and Otepää moraines. The average retreat rates of the ice margin of about 55 m/yr between the Gardno Phase and the Słupsk Bank Phase, and about 40 m/yr between the Słupsk Bank Phase and the Southern Middle Bank Phase suggest that the last deglaciation did not accelerate after the Gardno Phase when an extensive ice-dammed lake was formed in front of the retreating ice sheet. The ice margin was probably grounded rather than floating, which prevented its more rapid retreat. The timing of the two main ice margin stillstands at the Słupsk Bank and at the Southern Middle Bank corresponds to the cool periods around 15 and 14 ka interpreted from paleotemperatures of Greenland based on ice core GISP2. This suggests that the main phases of the last deglaciation in the southern Baltic region were at least partly triggered by climatic fluctuations in the Northern Hemisphere.

Keywords: deglaciation, Bayesian modeling, Baltic basin, Scandinavian Ice Sheet

1. Introduction

A significant warming of climate in the Northern Hemisphere at the Last Glacial Termination triggered the retreat of the Scandinavian Ice Sheet (SIS) (e.g., Denton et al., 2010; Lambeck et al., 2010; Cuzzone et al., 2016; Hughes et al., 2016; Stroeven et al., 2016; Patton et al., 2017). After the Last Glacial Maximum (LGM), which in the northern continental Europe occurred between ~24 and ~18 ka (e.g., Ehlers et al., 2011; Hughes et al., 2016; Hughes et al., 2021), the southern margin of the last SIS receded gradually, leaving glacial landforms and sediments clearly visible in the landscape. The timing of the last SIS retreat has recently been reconstructed from extensive datasets of available geochronological data and geomorphological/geological evidence constraining the ice sheet advance and retreat compiled into a GIS system (e.g., Hughes et al., 2016; Stroeven et al., 2016). Moreover, the last deglaciation of the entire Eurasian Ice Sheet complex was also modeled by the thermomechanical approach validated against the available geochronological data on ice margin fluctuations (e.g., Patton et al., 2017). However, the geochronological constraints used in reconstructions and modeling come mainly from terrestrial settings, leaving marine areas much less recognized in terms of dating sites significant for the timing of the ice margin retreat.

During deglaciation, the last SIS formed distinct ice-marginal belts, traditionally ascribed to the three main phases of the last glaciation in Germany and Poland: Brandenburg, Frankfurt, and Pomeranian (Woldstedt, 1925, 1935). The local LGM occurred during the Brandenburg (Leszno) Phase (~24–23 ka) in Germany and western Poland, and later during the Frankfurt (Poznań) Phase (~19 ka) in eastern Poland and Belarus (Marks, 2012, 2015). The subsequent ice-margin stillstand of the Pomeranian Phase is currently dated at ca. 17–16 ka (Marks, 2012) or 18–17 ka (Stroeven et al., 2016). This chronology has recently been established mainly by interpretation of calibrated radiocarbon ages (e.g., Marks, 2012), OSL dating (e.g., Wysota et al. 2009), and cosmogenic nuclide dating (e.g., Rinterknecht et al, 2006; Tylmann et al., 2019). However, much less is known about the timing of deglaciation phases along the present Baltic coast and within the southern Baltic basin. The chronology of the last deglaciation in the southern Baltic area was interpreted mostly from uncalibrated radiocarbon ages of organic sediments significant for constraining ice sheet advances and retreats, and the time-space correlation of relict ice-marginal landforms occurring on the southern Baltic floor with moraines in southern Sweden as well as in Lithuania, Latvia, and Estonia (e.g., Lundqvist, 1986; Rotnicki, Borówka, 1995; Uścinowicz, 1995, 1996, 1999;

Mojski, 1995, 2000; Marks 2002). As a consequence, the Gardno Phase was estimated at 14.5–13.8 ka BP, the Słupsk Bank Phase at 13.5–13.2 ka BP, and the Southern Middle Bank Phase at 13.0–12.8 ka BP. Later, those ages were calibrated to calendar years as 16.8–16.6 cal ka BP, 16.2–15.8 cal ka BP and 15.4–15.0 cal ka BP, respectively (e.g., Marks et al., 2016), although they seem too old and partly in conflict with the age of the Pomeranian Phase (17–16 ka) postulated by Marks (2012). The age of the Southern Middle Bank Phase was also corrected to 14.5 ka, according to newer, calibrated ^{14}C and ^{10}Be ages from southern Scandinavia, and the Słupsk Bank Phase was located between 15.5 and 14.5 ka (Uścinowicz, 2014). Recently, the age of the ice-margin stillstand of the Słupsk Bank Phase has been interpreted at ~15.2 ka on the basis of the OSL dating of glaciofluvial and glaciolacustrine deposits (Uścinowicz et al., 2019).

Despite the available geochronological data, the timing of the last deglaciation phases in this region and the correlation of subaqueous glacial landforms with terrestrial moraines are still problematic. The incomplete morphological record of particular ice margin positions and the inconsistency of the available dating constraints with morphostratigraphy make it difficult to establish any time-space correlations of the ice margin positions and to create time-slice reconstructions of the ice sheet (cf. Lüthgens, Böse, 2011; Marks, 2015; Hughes et al., 2016). Our motivation for this contribution was to tackle these problems with a Bayesian approach to constraining the chronology of the last deglaciation in the southern Baltic area. The goal of the article is to propose a new chronology of the retreat of the last SIS in the southern Baltic basin based on the available geochronological data and morphostratigraphy. Here, we present a reconstruction of the ice margin retreat within a sector of the last SIS located in the southern Baltic basin.

2. Study area and geochronological constraints

The study area is located in the southern part of the Baltic basin and in the northern fringe of Poland (Fig. 1A and B). It covers a part of the Polish middle-coast area with conspicuous moraines of the Gardno Phase and a part of the southern Baltic seafloor with ice-marginal landforms of the Słupsk Bank Phase and the Southern Middle Bank Phase (Fig. 1B). The Gardno moraines are end moraine ridges clearly defined in the landscape, recording the ice-margin position after a local ice sheet re-advance during the Gardno Phase (e.g., Bülow, 1924; Giedrojć-Juraha, 1949; Petelski, 1985; Jasiewicz, 1999).

The morphology of the Baltic Sea floor north of the Gardno moraines is characterized by bulges oriented WSW-ENE (Słupsk Bank, Stilo Bank and Southern Middle Bank) separated by two linear depressions: an unnamed depression and the Słupsk Furrow. The Bornholm Basin limits the Słupsk Bank and the Southern Middle Banks from the west, whereas the Gdańsk Basin and the Eastern Gotland Basin limit them from the east (Fig. 1B).

Landforms and deposits formed in the Baltic basin during deglaciation were partly or completely destroyed by erosion due to southern Baltic transgression during the Holocene and/or became masked by marine sediments. However, some of them are still reflected in the seafloor morphology. Relicts of ice-marginal landforms occur in the area of the Słupsk Bank and the Southern Middle Bank at a depth of 16–30 m, recording the ice-margin stillstand during deglaciation after the Gardno Phase (Uścinowicz, 1995, 1996, 1999). They are correlated with the Słupsk Bank Phase and the Southern Middle Bank Phase of the last deglaciation in the southern Baltic area (Fig. 1B). Relicts of end moraines, ground moraines, boulder fields, glaciofluvial deltas, and ice-marginal lake plains were found on the Słupsk Bank (Pikies, 1995; Uścinowicz, 1999). Numerous remnants of end moraine ridges up to 10–14 m high with slope angles of 5–7° and a SW-NE orientation of the long axis occur in the western part of this ice-marginal zone (Kramarska, 1991a, b). There are also smaller ridges on the northern slope of the Słupsk Bank interpreted as De Geer moraines (Uścinowicz, 2010). The area of the Southern Middle Bank also consists of relicts of glaciofluvial deltas and ground moraine (Pikies, 1995; Uścinowicz, 1999).

Radiocarbon dates available for the southern Baltic region indicate the age of sediments postdating the last deglaciation in the range of 17.50 ± 0.24 – 9.75 ± 0.27 ka b2k (Fig. 1B, Tab. S1). Most of these dates (16 out of 23) fall into the range of 14.68 ± 0.45 – 12.00 ± 0.25 ka b2k, indicating the Late Glacial age. Four ages predate the Late Glacial period (17.50 ± 0.24, 17.15 ± 0.33, 16.77 ± 0.39, and 15.45 ± 0.55 ka b2k), and three dates are from the Holocene sediments (11.45 ± 0.20, 9.92 ± 0.20 and 9.75 ± 0.27 ka b2k). The oldest radiocarbon ages come from the Gardno moraines region (17.50 ± 0.23 and 16.77 ± 0.39 ka b2k) and the Pomeranian Bay (17.15 ± 0.33 and 15.45 ± 0.55 ka b2k). Ages older than 15.45 ka b2k are not confirmed by palynological data and are most probably overestimated due to redeposition of older organic matter (Uścinowicz et al., 2019). They may indicate, however, that organic sediments are not older than these overestimated radiocarbon dates. Luminescence dates of mineral sediments are available for the area between the Gardno and Słupsk Bank moraines and for the Southern Middle Bank (Fig. 1B). They come from glaciofluvial deltas and ice-marginal lake deposits or coastal ridges, and may be used to constrain deglaciation chronology, since glaciofluvial deltas and ice-marginal lakes are correlated with particular phases of the ice sheet retreat (Uścinowicz et al., 2019). OSL dates of glaciofluvial deltas on the Słupsk Bank range from 9.77 ± 0.83 to 21.30 ± 2.00 ka, whereas OSL dates of ice-marginal lake sediments deposited in front of the Słupsk Bank cover an extremely large spectrum of ages: from 11.09 ± 0.79 to 135.0 ± 12.0 ka. Sediments on coastal ridges in the Gardno-Łeba Lowland north east of the Gardo moraines and interpreted as morphological evidence of the southern extent of an ice-marginal lake formed south of the Słupsk Bank range from 11.03 ± 0.73 to 16.13 ± 0.94 ka (Uścinowicz et al., 2019). One TL date is available for glaciofluvial sand overlying till on the southern Middle Bank, and it shows the age of this sand to be 13.20 ± 2.00 ka (Kramarska et al., 1990).

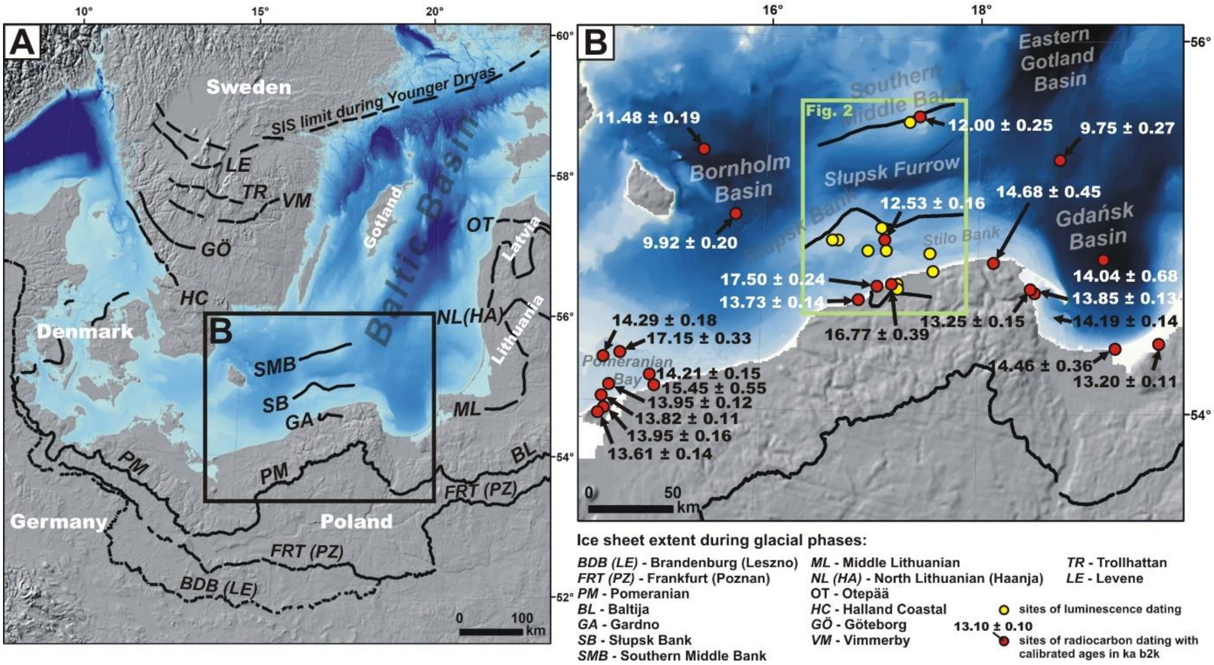

Fig. 1. Study area and dating sites. (A) The extent of the Scandinavian Ice Sheet (SIS) in the southern and central Baltic Sea region during particular phases of the last deglaciation. (B) The southern part of the Baltic basin with sites of sediment dating, the main morphological units of the seafloor and the area of Bayesian age modeling (green rectangle). The conventional ^{14}C ages were calibrated according to the *IntCal20* calibration curve (Reimer et al., 2020). For details see Tab. S1 in Supplementary Materials.

3. Materials and methods

The sites of sediment dating that were used in the Bayesian analysis are located in the Gardno-Łeba Lowland close to the ice marginal zone of the Gardno Phase and on the southern Baltic seafloor close to the ice marginal zones of the Słupsk Bank Phase and the Southern Middle Bank Phase (Fig. 2). Radiocarbon dates were obtained from 2 sites in the Gardno-Łeba Lowland, whereas luminescence dates come from sediments cored within the Southern

Middle Bank, the Słupsk Bank, and seafloor depressions south of the Słupsk Bank (Fig. 2A), and from sediments on coastal ridges in the Gardno-Łeba Lowland (Fig. 2B and C).

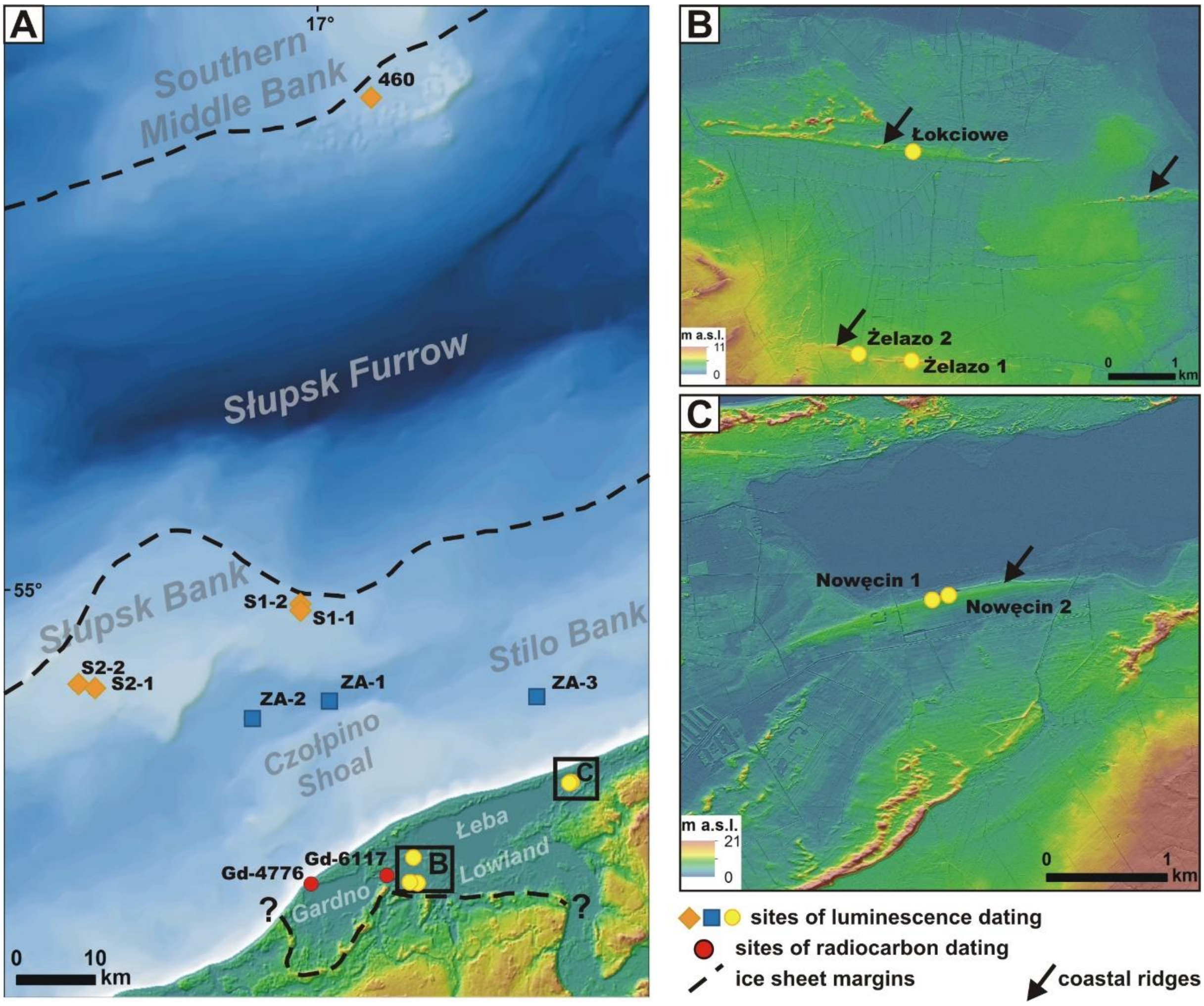

Fig. 2. Sites of radiocarbon and luminescence dating used in Bayesian modeling. (A) Location of luminescence and radiocarbon dating sites against the morphology of land and seafloor, and the main margins of the last SIS. (B and C) Detailed location of luminescence dating sites on coastal ridges of the ice marginal lake correlated with the Słupsk Bank Phase (Uścinowicz et al., 2019).

The chronology of deglaciation was modeled on the basis of the two oldest radiocarbon ages of sediments overlying the boulder pavement interpreted as remnants of till in the Gardno-Łeba Lowland (Rotnicki, Borówka, 1995), 26 OSL ages of glaciofluvial, glaciolacustrine, and coastal ridge deposits (Uścinowicz et al., 2019), and one TL age of glaciofluvial sand (Kramarska et al., 1990) (Tab. 1). Radiocarbon ages are based on conventional Liquid Scintillation Counter (LSC) measurements of bulk organic samples taken at the Gliwice Radiocarbon Laboratory (Rotnicki, Borówka, 1995). The conventional ^{14}C ages were calibrated with OxCal 4.4 according to the *IntCal20* calibration curve (Reimer et al., 2020). OSL ages are based on opto-luminescence measurements of 90-125 µm quartz grains taken at the Gliwice Luminescence Laboratory using the single-aliquot regenerative-dose

(SAR) protocol for determination of equivalent doses for individual aliquots (Uścinowicz et al., 2019). The Central Age Model (CAM) was used to calculate equivalent doses for particular samples on the basis of aliquot distribution (Galbraith et al., 1999). TL age is based on thermoluminescence measurements of 80–110 µm quartz grains taken at the University of Gdańsk Luminescence Laboratory using the regenerative-dose protocol (Kramarska et al., 1990). Moreover, to additionally constrain our chronological model, we used the available literature data related to the timing of (1) the Pomeranian Phase in Poland (Marks, 2012; Stroeven et al., 2016) and (2) the deglaciation of Gotland (Anjar et al., 2014).

We used 26 out of 33 available OSL ages of genetically diversified sand, gravel, and silt in the southern Baltic area correlated with the Słupsk Bank Phase (Uścinowicz et al., 2019; Tab. S2), which resulted from a preliminary selection based on their distribution and identification of 7 outliers (Fig. 3). The latter refer to glaciolacustrine sediments from an ice-marginal lake and are clearly overestimated, probably due to an incomplete bleaching of sediment grains during their transport and deposition (Uścinowicz et al., 2019). The age range of the 26 OSL dates used in the modeling of the chronology is from 9.77 ± 0.83 to 21.30 ± 2.00 ka, whereas the range of dates identified as outliers and not included in the modeling is from 37.10 ± 2.40 to 135.0 ± 12.0 ka (Fig. 3).

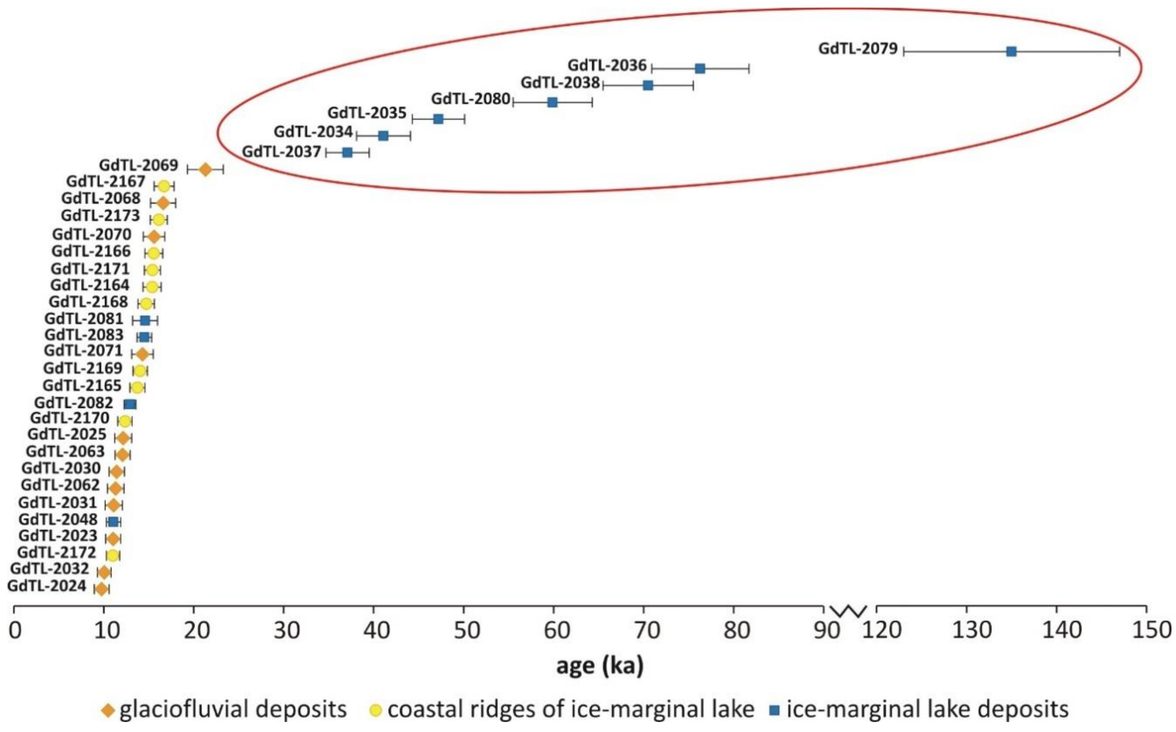

Fig. 3. OSL dates of glaciofluvial, glaciolacustrine deposits from the Słupsk Bank and seafloor depressions south of the Słupsk Bank, and from sediments on coastal ridges in the Gardno-Łeba Lowland. Deposition of these sediments is correlated with the ice-margin stillstand of the Słupsk Bank Phase (Uścinowicz et al., 2019). The red oval indicates the oldest ages, which are most probably

overestimated because of the poor bleaching of sediments grains and were not included in the Bayesian analyses. For details see Tab. S2 in Supplementary Materials.

The Bayesian approach to modeling the chronology of deglaciation uses the morphostratigraphic record and geochronological constraints of ice-margin retreat (e.g., Chiverrell et al., 2013). The *prior* model (using Bayesian nomenclature) consists of the history of ice-margin positions arranged in the order of ice margin retreat inferred from geomorphology and stratigraphy (Fig. 4A). Numerical dating controls (age probability distributions) constrain the possible time of ice-margin positions (Fig. 4B). In Bayesian modeling, they represent the *likehood* that any one sample has a particular age. Age modeling was performed using *Sequence* algorithms in OxCal (Bronk Ramsey, 2009a), ver. 4.4. The algorithms use Markov chain Monte Carlo (MCMC) sampling to build a distribution of possible solutions and generate a probability called the *posterior* density estimate for each sample. It is a result of both the *prior* model and the *likehood* probability. These density estimates take into account the chronological order (*prior*) and typically reduce the uncertainty range in comparison to *likehood* probabilities (Chiverrell et al., 2013).

4. Construction of the chronological model

The deglaciation chronology was inferred from a hypothetical "relative-order" model of the expected chronological order with events arranged into a pseudo-stratigraphical order reasoned solely from landform-sediment relationships independent of the numerical dating controls (Fig. 4). The *Sequence* model in OxCal was divided into a series of *Phases*, each representing the stages of deglaciation in the analyzed region which may be correlated with particular dating controls. Thus, each *Phase* consists of a group of dating controls and is separated by *Boundary* commands, which delimit the duration of each *Phase* and generate an age *posterior* density estimate. Moreover, we used *After* ("*terminus post quem*") and *Before* ("*terminus ante quem"*) commands to constrain the chronology when stages evidently post-date or pre-date particular events. The whole *Sequence* is constrained by *Boundary* commands, which delimit the start and the end of the model (Fig. 4A).

The start of the *Sequence* was defined by the age of the Pomeranian Phase, which based on recent estimates for northern Poland (Marks, 2012; Stroeven et al., 2016) may be roughly constrained to 18–16 ka. Then, the "Gardno Phase" was introduced (*Boundary*) with the constraint that it must post-date (*After*) the Pomeranian Phase. The Phase "post-Gardno" consists of radiocarbon ages (Gd-4776 and Gd-6117) from the oldest organic deposits overlying the boulder pavement being a remnant of till correlated to the last ice advance in the

Gardno-Łeba Lowland (Figs. 2A, and 4B). Subsequently, the “Słupsk Bank Phase” was introduced with *Boundary* and *Phase* consisting of a group of OSL dating controls (GdTL samples) from glaciofluvial deltas, ice-marginal lake deposits, and coastal ridge sediments (Uścinowicz et al., 2019). Then, the later stage of deglaciation, the “Southern Middle Bank Phase” was defined with a *Boundary* command as well as *Phase* consisting of one TL date (UG-793) of glaciofluvial sediments occurring on the Southern Middle Bank (Fig. 4A and B). The constraint was that it had to pre-date (*Before*) the most likely timing of the deglaciation of Gotland (13.7–12.3 ka) based on recalculated surface exposure ^{10}Be ages of Anjar et al. (2014). The *Sequence* is closed with the *Boundary* “End” command. The notation of commands used to process the algorithms is available in the Supplementary Materials of the article (Tab. S3).

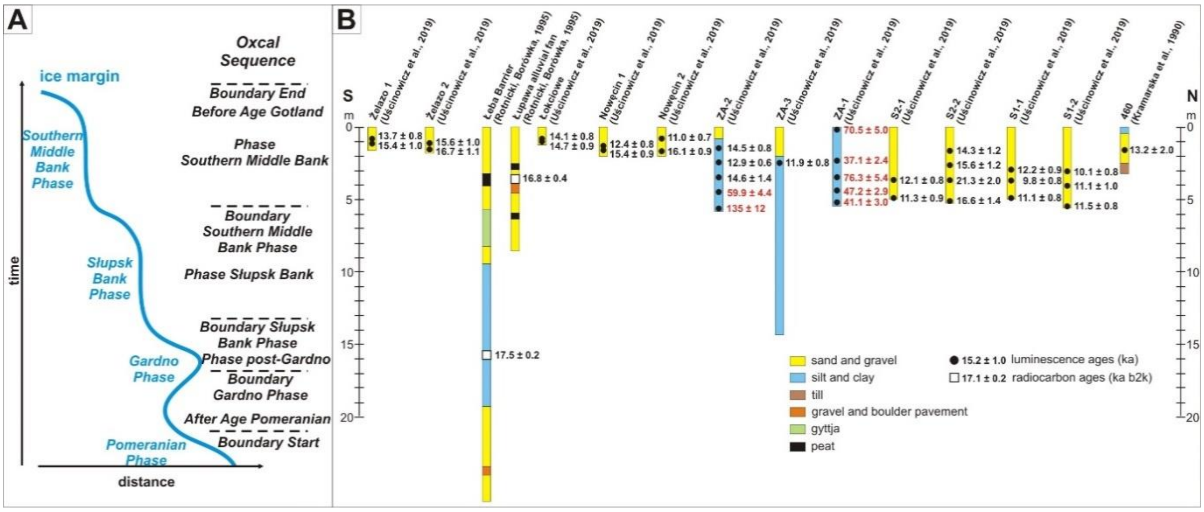

Fig. 4. Illustration of the morphostratigraphic record and geochronological constraints of the ice-margin retreat used in the Bayesian modeling. (A) Schematic time-distance diagram representing fluctuations of the last SIS margin in the southern Baltic area and the structure of the OxCal *Sequence* model. (B) Lithostratigraphic context of radiocarbon and luminescence ages used in the Bayesian modeling. References to the original publications with ^{14}C and luminescence dates are given above schematic sediment logs. Luminescence ages treated as outliers and not included in the model (see Fig. 3) are marked in red.

The run of the *Sequence* model was conducted in the *Outlier* mode, which assumes that outliers are distributed according to a student T distribution with 5 degrees of freedom; the scale is allowed to lie anywhere between 10^0 to 10^4 years (Bronk Ramsey, 2009b). In the initial model, the dating controls were all entered with a prior probability of 0.05 of being an outlier. Ages that clearly do not fit the model (characterized by the agreement index with the model A < 10%) were treated as outliers and removed. We discuss ages identified as outliers and possible reasons of their incompatibility with the model below. Ages having a much higher agreement index with the initial model, but not higher than 60%, and exceeding the

0.05 threshold of probability of being outliers in the initial model results, were down-weighted by being assigned a prior probability of 0.75 of being outliers. Then, a re-run of the same *Sequence* model was conducted for the chronological sequence without outliers and with down-weighted ages. Finally, the agreement index for the re-run model (A_{model}) was used to evaluate the reliability of the chronological sequences obtained (Chiverrell et al., 2013). Both input ages and modeled ages were reported with 1 σ uncertainty (68.2% probability).

5. Results

The model based on the assumed sequence of events and all dating controls (Tab. 1, Fig. 4A) showed a very poor agreement index A_{model} = 0.5%. This suggested that the results of the initial *Sequence* were not reliable and some outliers and problematic ages must occur among the dating controls. We identified 10 outliers with the individual agreement index A < 10% (Tab. 1). One radiocarbon date belonging to the *Phase* "post-Gardno" (sample Gd-4776) showed a low agreement index of 5.3%. The calibrated age of this sample is 17.50 ± 0.24 ka b2k, and it is most probably too old an age for the post-Gardno phase, which may result from the redeposition of organic matter and the contamination of this sample with older carbon. It is highly probable because a bulk sample of organic material dispersed in ice-dammed lake clay and silt was dated (Rotnicki, Borówka, 1995). Moreover, no additional data supporting the apparent age of these samples (e.g. palynology) are available. Nine out of twenty-six OSL ages belonging to the *Phase* "Słupsk Bank" (samples GdTL) also had very low agreement indexes ranging between 3.9 and 9.2%. Most of these ages are too young (between 9.77 ± 0.83 ka and 11.45 ± 0.84 ka), which may result from a partial or total bleaching of grains after their deposition in the period of dead-ice blocks melting, just before and during marine transgression (Uścinowicz et al., 2019). The age of one sample is too old (21.30 ± 2.00 ka), which is most probably the result of an incomplete bleaching of grains during glaciofluvial transport. We also identified 3 OSL ages belonging to the *Phase* "Słupsk Bank" (samples GdTL) that had an agreement index with the initial model in the range of 33.6 to 47.6%. These are OSL ages 12.35 ± 0.80, 12.16 ± 0.94, and 12.10 ± 0.83 ka, which are slightly too young within the *Sequence* (Tab. 1). The causes of the insufficient compatibility of these dates with the model could be similar to the ones mentioned above when analyzing outliers with very low agreement indexes (partial or total bleaching of grains after their deposition). Thus, they were down-weighted by being assigned a prior probability of 0.75 of being outliers.

Tab. 1. Dating controls and results of the Bayesian age modeling.

Boundary/Phase	**Sample**	**Age (ka b2k/ka)**	**Initial model (A_{model} = 0.5 %)**		**Model without outliers and with down-weighted ages (A_{model} = 100.0%)**	
			Modeled age (ka)	**A index (%)**	**Modeled age (ka)**	**A index (%)**
Southern Middle Bank	UG-793	13.20 ± 2.00	13.11 ± 0.17	144.6	13.62 ± 0.47	136.7
Southern Middle Bank					**13.88 ± 0.50**	-
Słupsk Bank	GdTL-2173	16.13 ± 0.94	15.11 ± 0.70	81.5	15.06 ± 0.56	76.2
	GdTL-2172	*11.03 ± 0.73*	*14.14 ± 0.82*	*4.7*	-	-
	GdTL-2171	15.42 ± 0.90	14.89 ± 0.69	103.6	14.92 ± 0.55	109.3
	GdTL-2170	12.35 ± 0.80*	13.65 ± 0.47	47.6	14.46 ± 0.63	98.1
	GdTL-2169	14.05 ± 0.79	14.19 ± 0.60	115.8	14.50 ± 0.51	108.8
	GdTL-2168	14.72 ± 0.92	14.55 ± 0.69	114.2	14.72 ± 0.54	124.5
	GdTL-2167	16.70 ± 1.10	15.14 ± 0.74	61.2	14.95 ± 0.61	91.7
	GdTL-2166	15.56 ± 0.98	14.90 ± 0.72	101.8	14.92 ± 0.56	106.3
	GdTL-2165	13.73 ± 0.84	14.05 ± 0.58	116.7	14.43 ± 0.51	95.9
	GdTL-2164	15.38 ± 1.00	14.82 ± 0.72	106.4	14.88 ± 0.56	113.8
	GdTL-2048	*11.09 ± 0.79*	*14.01 ± 0.80*	*4.6*	-	-
	GdTL-2081	14.60 ± 1.40	14.49 ± 0.77	126.5	14.71 ± 0.59	132.4
	GdTL-2082	12.92 ± 0.64	13.63 ± 0.41	83.9	14.21 ± 0.53	34.5
	GdTL-2083	14.51 ± 0.81	14.48 ± 0.65	112.9	14.65 ± 0.52	120.8
	GdTL-2068	16.60 ± 1.40	14.96 ± 0.78	75.3	14.97 ± 0.60	74.1
	GdTL-2069	*21.30 ± 2.00*	*14.96 ± 0.88*	*3.9*	-	-
	GdTL-2070	15.60 ± 1.20	14.81 ± 0.76	105.0	14.88 ± 0.58	111.6
	GdTL-2071	14.30 ± 1.20	14.39 ± 0.73	124.0	14.65 ± 0.57	125.9
	GdTL-2062	*11.33 ± 0.91*	*13.76 ± 0.65*	*9.2*	-	-
	GdTL-2063	12.10 ± 0.83*	13.65 ± 0.49	33.6	14.46 ± 0.63	97.3
	GdTL-2030	*11.45 ± 0.84*	*13.75 ± 0.66*	*8.78*	-	-
	GdTL-2031	*11.11 ± 0.97*	*13.79 ± 0.67*	*7.6*	-	-
	GdTL-2032	*10.06 ± 0.76*	*14.28 ± 0.80*	*5.4*	-	-
	GdTL-2023	*11.05 ± 0.84*	*13.95 ± 0.78*	*4.7*	-	-
	GdTL-2024	*9.77 ± 0.83*	*14. 28 ± 0. 80*	*5.4*	-	-
	GdTL-2025	12.16 ± 0.94*	13.70 ± 0.50	45.0	14.47 ± 0.63	95.1
Słupsk Bank					**15.59 ± 0.58**	-
post-Gardno	Gd-6117	16.77 ± 0.39	16.45 ± 0.35	97.8	16.26 ± 0.46	77.2
	Gd-4776	*17.50 ± 0.24*	*16.38 ± 0.50*	*5.3*	-	-
Gardno					**16.49 ± 0.47**	-

Italics - ages identified in the *Sequence* as outliers. See text for explanation.
* ages down-weighted in the *Sequence* to a prior probability of 0.75 of being outliers. See text for explanation.

After removing outliers, the model based on the same chronological sequence and 19 dating controls (17 OSL, one ^{14}C, and one TL) with 3 OSL ages down-weighted showed a much better agreement index A_{model} = 100.0%. The individual agreement index for the modeled ages ranges between 34.5 and 136.7%, but only one ages have A < 60% (Tab. 1).

The modeled age distribution for the Gardno Phase is 16.49 ± 0.47 ka. The results show that the possible age of the Słupsk Bank Phase may be constrained to 15.59 ± 0.58 ka and the modeled age for the Southern Middle Bank Phase is 13.88 ± 0.50 ka (Tab. 1). Assuming this time frame for the last deglaciation of the southern Baltic basin and for the spatial distribution of the main ice-marginal landforms, a rough estimation of the average retreat rate of the ice sheet front was proposed (Fig. 5). The retreat rate was probably about 55 m/yr between the Gardno Phase and the Słupsk Bank Phase, and about 40 m/yr between the Słupsk Bank Phase and the Southern Middle Bank Phase.

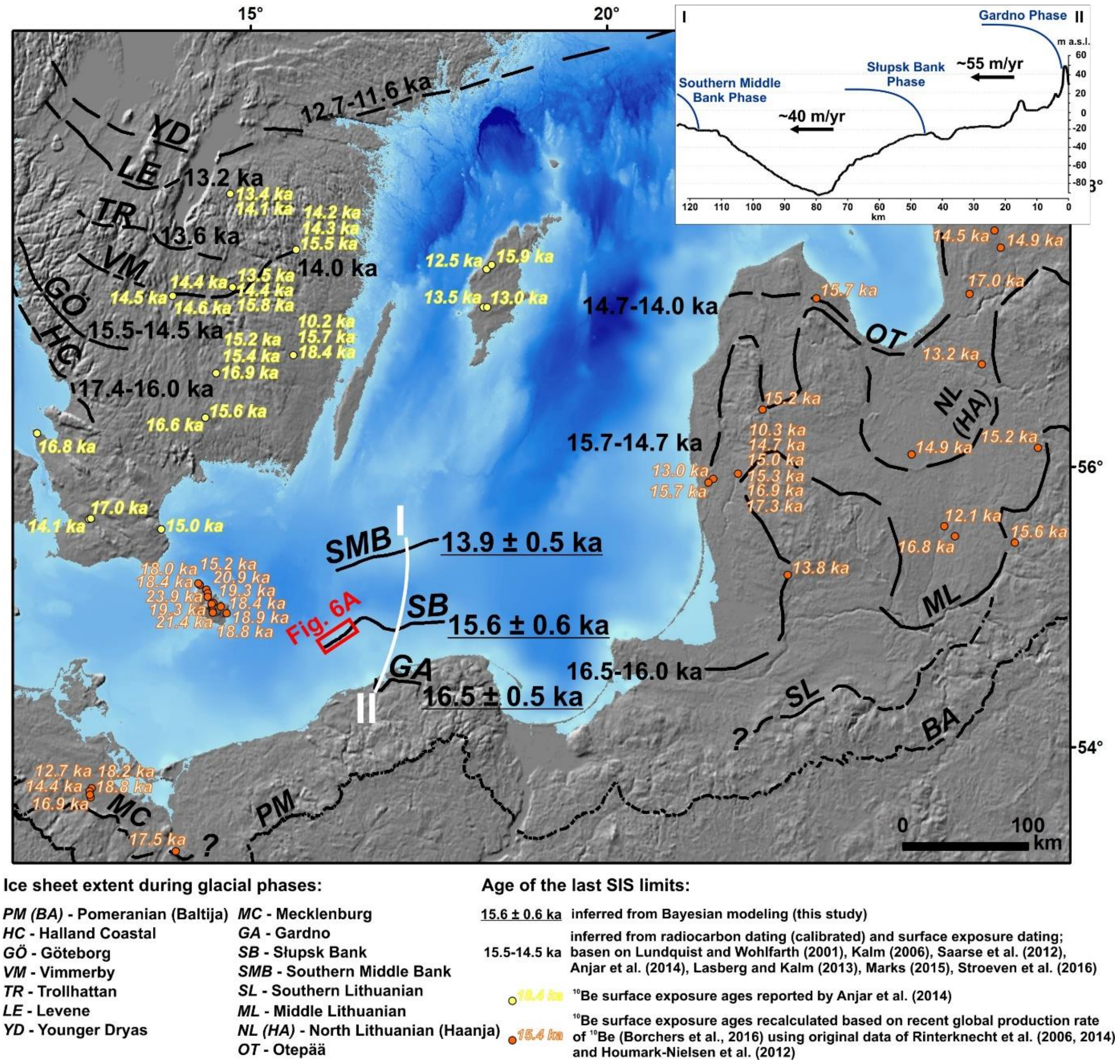

Fig. 5. Age of ice margin stillstands during the last SIS deglaciation phases in the southern Baltic basin and surroundings. Modeled ages of ice-margin positions are given, and the estimated retreat rate of the ice sheet front between the Gardno, Słupsk Bank, and Southern Middle Bank phases are shown. Ages of ice margin positions in southern Sweden are given according to Anjar et al. (2014) and Stroeven et al. (2016). Ages of ice margin positions in Lithuania and Latvia according to Kalm (2006) and Saarse et al. (2012).

6. Discussion

6.1. Age of deglaciation phases and space-time correlation

The modeled age of 16.5 ± 0.5 ka for the ice margin of the Gardno Phase indicates a rather rapid ice re-advance after the deglaciation of northern Poland from the Pomeranian

Phase ice sheet limit, probably ~18–17 ka (Stroeven et al., 2016). This timing for the Gardno Phase is comparable with recent results of Uścinowicz et al. (2019), in which its possible age is estimated at 16.0–15.5 ka, and interpretation of Marks et al. (2016) who proposed its possible age 16.8–16.6 cal ka BP. The age of Gardno moraines modeled in this paper is slightly older than the age of the Halland Coastal moraines in southern Sweden given by Houmark-Nielsen (2008) as 16–15 ka, and similar to about 17.4–16.0 ka proposed by Stroeven et al. (2016) (Fig. 5). Therefore, the space-time correlation of the Gardno moraines with the Halland Coastal moraines seems to be the most reliable, and the ice margin ran from the Gardno moraines possibly through the North Rügen moraines to the north-west. The continuation of the marginal belt of the Gardno moraines to the east and north-east is less clear. The Pomeranian moraines are most often correlated with the Baltija moraines (e.g., Lasberg, 2014; Marks 2015; Marks et al., 2016), and the moraines of the Mecklenburg Phase in NE Germany could probably be linked to the South Lithuanian moraines, so the Gardno ice-marginal belt most probably corresponds to the moraines of the Middle Lithuanian Phase, as earlier suggested by Raukas et al. (1995). Timing of deglaciation in the region of the Middle Lithuanian moraines was previously estimated at about 16.5–16.0 ka (Lasberg, Kalm, 2013) what is also similar to our modeling constraint for the Gardno Phase.

The modeled ages of the ice margin stillstands during the subsequent Słupsk Bank Phase (15.6 ± 0.6 ka) and the Southern Middle Bank Phase (13.9 ± 0.5 ka) are likewise overlapping with results presented by Uścinowicz (2014) and Uścinowicz et al. (2019): ~15.2 ka and ~14.5 ka, respectively. These ice margin limits may be correlated with the southern Swedish Göteborg and Vimmerby moraines, recently dated on the basis of calibrated radiocarbon and ^{10}Be surface exposure ages to about 15.5–14.5 ka and 14 ka, respectively (e.g., Lundqvist, Wohlfarth, 2001; Anjar et al., 2014; Stroeven et al., 2016), and with the North Lithuanian (Haanja) and Otepää moraines to the east, where the age of this ice marginal belts may be constrained to 15.7–14.7 ka and 14.7–14.0 ka, respectively (Kalm, 2006; Saarse et al., 2012; Marks, 2015).

6.2. Ice margin retreat rate

We calculated the average retreat rate of the ice margin at ~55 m/yr between the Gardno Phase and the Słupsk Bank Phase, and ~40 m/yr between the Słupsk Bank Phase and the Southern Middle Bank Phase on the basis of the modeled ages of ice margin stillstands (Fig. 5). Stroeven et al. (2016) estimated the average retreat rate of the southern margin of the last SIS during the time period 17–13 ka at mostly 50–200 m/yr. The chronology and distribution of the southern Swedish moraine belts suggest that the average retreat rate of the ice margin there may have amounted to ~20 m/yr during deglaciation from the Halland Coastal to the Göteborg moraines, ~50 m/yr from the Göteborg to the Vimmerby moraines, ~85 m/yr from the Vimmerby to Trollhattan moraines, and also ~85 m/yr from the Trollhattan to the Levene moraines. It indicates acceleration of the retreat rate during progressive deglaciation of southern Sweden. Our estimation of the ice margin retreat rate for the Gardno, Słupsk Bank, and Southern Middle Bank Phases is similar to the average retreat rate of the margin of the last SIS in northern Poland, south of the Baltic basin, which may be estimated at ~50 m/yr. These calculations are based on recent geochronological constraints for the local LGM ice margin position in central and eastern Poland ~22–18 ka (Tylmann, et al. 2019) and for the Pomeranian Phase ice margin stillstand ~18–17 ka (Stroeven et al., 2016). The retreat rate between Pomeranian Phase and Gardno Phase ice margin stillstands (~17.5 ka to ~16.5 ka) was slightly higher, and it may have amounted to at least ~70 m/yr. However, these results suggest that the retreat rate of the ice margin was relatively stable from the early stages of deglaciation after the local LGM, to the later stages of the ice sheet recession in the Baltic basin. The lack of a clear acceleration of the ice margin retreat rate in the Baltic basin compared to that in northern Poland indicates that, despite the formation of an extensive ice-dammed lake in front of the retreating ice sheet after the Gardno Phase (Uścinowicz, 1995, 1999), the ice sheet margin was still grounded rather than floating. This may have prevented a more rapid recession, characteristic of a floating ice front, which usually amounts to hundreds or even thousands of meters per year (c.f., Dowdeswell et al., 2020). This situation probably persisted until the Southern Middle Bank Phase. Moreover, the retreat did not accelerate within the southern Baltic, as it was the case in the southern Sweden, probably also due to much thicker ice infilling southern Baltic basin in comparison to the southern Scandinavia.

An independent proxy for the ice margin retreat rate in the southern Baltic basin may be a geomorphological record available on the NW slope of the Słupsk Bank. A DTM obtained by the multibeam echosounding of this area reveals numerous moraine ridges with a distinctive spatial distribution and morphology (Fig. 6). These are relicts of closely spaced sub-parallel ridges orientated mainly NE-SW (Fig. 6A) and usually characterized by asymmetric cross profiles with steeper SE slopes (Fig. 6B). This system of ridges was interpreted as a remnant of De Geer moraines, which indicate a subaqueous type of deglaciation after the ice margin stillstand of the Słupsk Bank Phase (Uścinowicz 2010). The main arguments supporting the De Geer moraine interpretation of these ridges are as follows: (1) the regular spatial arrangement of closely spaced asymmetric ridges; (2) their morphometric parameters similar to those of typical De Geer moraines (up to hundreds of meters long, tens of meters wide, up to 10 m high, and spaced from tens to hundreds of meters apart); (3) their geological structure with boulders/cobbles on the top and till inside (Uścinowicz, 2010). We used them to estimate the possible retreat rate of the ice margin, assuming that this kind of moraines may have been formed annually (e.g., Bouvier et al, 2015; Sinclair et al., 2018). The distance between particular ridges varies from tens to hundreds of meters, and smaller ridges are usually spaced more closely (~60–90 m apart) than bigger ridges (mostly ~100–300 m apart). Moraines located to the NW of the main moraine belt correlated with the Słupsk Bank Phase show a minimum distance of ~65–100 m between particular ridges and a distance of ~100–220 m between the main ridges (Fig. 6B). It suggests more rapid recession than our estimation of the average retreat rate of the ice margin after the Słupsk Bank Phase, that is ~40 m/yr (Fig. 5). The estimation based on the modeled ages of ice margin stillstands is only an approximation of the ice margin retreat rate, which in fact varied over time and space, as perhaps reflected by the diversified spacing of De Geer moraine ridges. However, the minimum distance between closely spaced ridges (~65 m) is a similar order of magnitude as the ice margin retreat rate constrained by our modeled chronology (40 m/yr), so we assume that the moraines may have been formed annually. Perhaps, not all ridges were preserved at the seafloor since deglaciation (they are relicts of glacial landforms), what may explain their wider spacing of hundreds of meters. So, the estimated average retreat rate of the ice sheet after the Słupsk Bank Phase is at least partly confirmed by the seafloor geomorphology preserved on the NW slope of the Słupsk Bank.

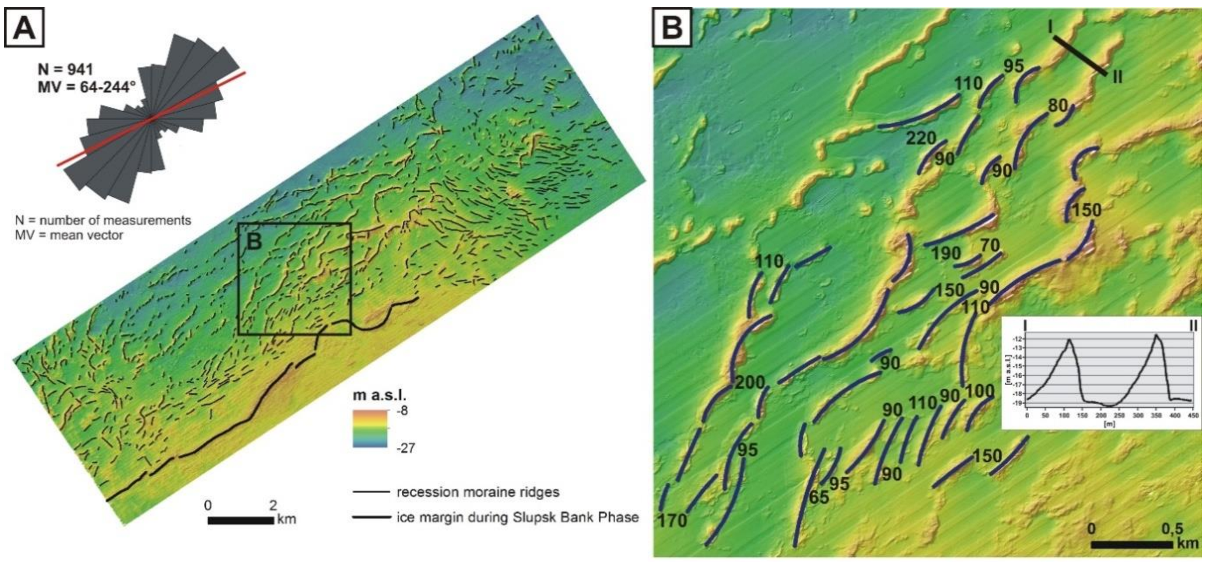

Fig. 6. Remnants of moraine ridges interpreted as De Geer moraines on the north-western slope of the Słupsk Bank. (A) Spatial distribution of moraine ridges. The orientation of their long axis is shown in the rose diagram with basic statistics (number of measurements and mean vector). (B) De Geer

moraines located to the north-west of the main moraine belt correlate with the Słupsk Bank Phase. Distances between particular ridges (dark blue lines) are shown in meters.

6.3. Time-slice reconstruction

Our modeling included calibrated radiocarbon ages, luminescence ages, and other chronological constraints (relative sequence, age of Pomeranian Phase, and deglaciation of Gotland). Therefore, the chronology obtained is based on more solid lines of evidence than previous interpretations of uncalibrated radiocarbon ages (e.g., Rotnicki, Borówka, 1995) and time-space correlations of ice margin positions (e.g., Lundquist, 1994; Lagerlund et al., 1995; Raukas et al., 1995; Uścinowicz, 1996, 1999). The proposed chronology of the SIS retreat and the space-time correlation of ice margin positions during particular phases of deglaciation in the southern Baltic region make it possible to propose a time-slice reconstruction of the ice sheet. We reconstructed the most probable configuration of the southern front of the SIS during the time period between 18-17 ka and 14 ka (Fig. 7).

About 18-17 ka, the SIS margin was located in northern Germany, northern Poland, and southern Lithuania along the Pomeranian moraines. The modeled age of 16.5 ± 0.5 ka for the ice margin re-advance of the Gardno Phase indicates a rather rapid re-advance after the deglaciation of northern Poland during the Pomeranian Phase. However, during the ice-sheet retreat from the Pomeranian moraines to the Gardno moraines there was at least one or two stillstands known as the Mecklenburg Phase (e.g., Lagerlund et al., 1995, Rinterknecht et al., 2014) or the Rosenthal Phase and the Velgast Phase (e.g., Hoffmann, 2002). A few minor local glacial marginal zones located between the Pomeranian and the Gardno moraines are also shown by Marks (2005) in Pomerania in Poland. This means that up to the Gardno Phase the southern Baltic basin was still infilled with ice (Fig. 7A). An important question arise, however, with regard to deglaciation of Bornholm. ^{10}Be surface exposure ages reported by Houmark-Nielsen et al. (2012) indicate the most likely timing of ice sheet retreat there between 17 and 16 ka. Mean ^{10}Be age calculated based on eight the most reliable ages from Bornholm was reported as 16.6 ± 0.9 ka (Anjar et al., 2014). However, based on the most recent global ^{10}Be production rate (Borchers et al., 2016) these ages are significantly older and mostly fall into the range 19–18 ka (Fig. 5). Using the recent Scandinavian reference ^{10}Be production rate (Stroeven et al., 2015) makes them ~2.8% older than ages calculated with the global ^{10}Be production rate. It is in conflict with age estimation for ice margin positions south and west of the Baltic basin (cf. Houmark-Nielsen, 2011; Marks, 2012; Stroeven et al., 2016; Tylmann et al. 2019), and also with chronology proposed in this research (Fig. 7). The reason could be that surface exposure ages from Bornholm are too old due to significant amount of inherited ^{10}Be occurring within particular ages, so that they do not indicate the actual timing of deglaciation there (cf. Houmark-Nielsen et al., 2012). Other scenario could be, if we assume the apparent ^{10}Be ages as good indicators of deglaciation chronology, that Bornholm massive remained ice free as a nunatak despite ice sheet advances between 18-17 ka and 15.5 ka. This scenario is, however, highly speculative as no other evidences about "nunatak history" of Bornholm was found so far.

Around 16.5 ka after a relatively rapid recession of the Pomeranian ice margin, the ice sheet re-advance reached the northernmost parts of the present Baltic coastline in Poland. The lobate ice margin during the Gardno Phase possibly ran from the Halland Coastal moraines on the west, across the northern edges of Rügen, the northern part of the Pomeranian Bay, the moraine arc in the middle Baltic coast of Poland, and the southern edges of the Gdańsk Basin, to the Middle Lithuanian Moraines on the east (Fig. 7B). Later, the ice margin progressively receded, and around 15.5 ka, during the Słupsk Bank Phase, the southern Baltic basin was occupied by an extensive ice lobe, which spread from the eastern coasts of southern Sweden to the western regions of Lithuania (Fig. 7C). The ice margin within the ice lobe was located up to ~200 km south of the ice margin beyond the lobe. The lobate configuration of the southern front of the SIS occurred also about 14.0 ka, when the ice margin retreated slightly to the north and was located on the Southern Middle Bank in the Baltic basin, on the Vimmerby moraines in southern Sweden, and on the Otepää moraines in the north-east (Fig. 7D).

The reconstruction proposed in this study shows two main stillstands of the receding ice margin in the southern Baltic basin during the Słupsk Bank and Southern Middle Bank Phases about 15.5 ka and 14.0 ka, respectively. An extensive ice lobe occupied the Baltic basin during these phases of deglaciation (Fig. 7C and D). This ice lobe was probably topographically constrained by the elongated depression of the Baltic basin and highly elevated moraine insular uplands in Lithuania and Latvia playing a crucial role. Moreover, the main ice streaming corridor of the last SIS, which was located along the Baltic depression (cf. Patton et al., 2017), may still have influenced the configuration of the receding ice margin during the deglaciation of the southern Baltic basin.

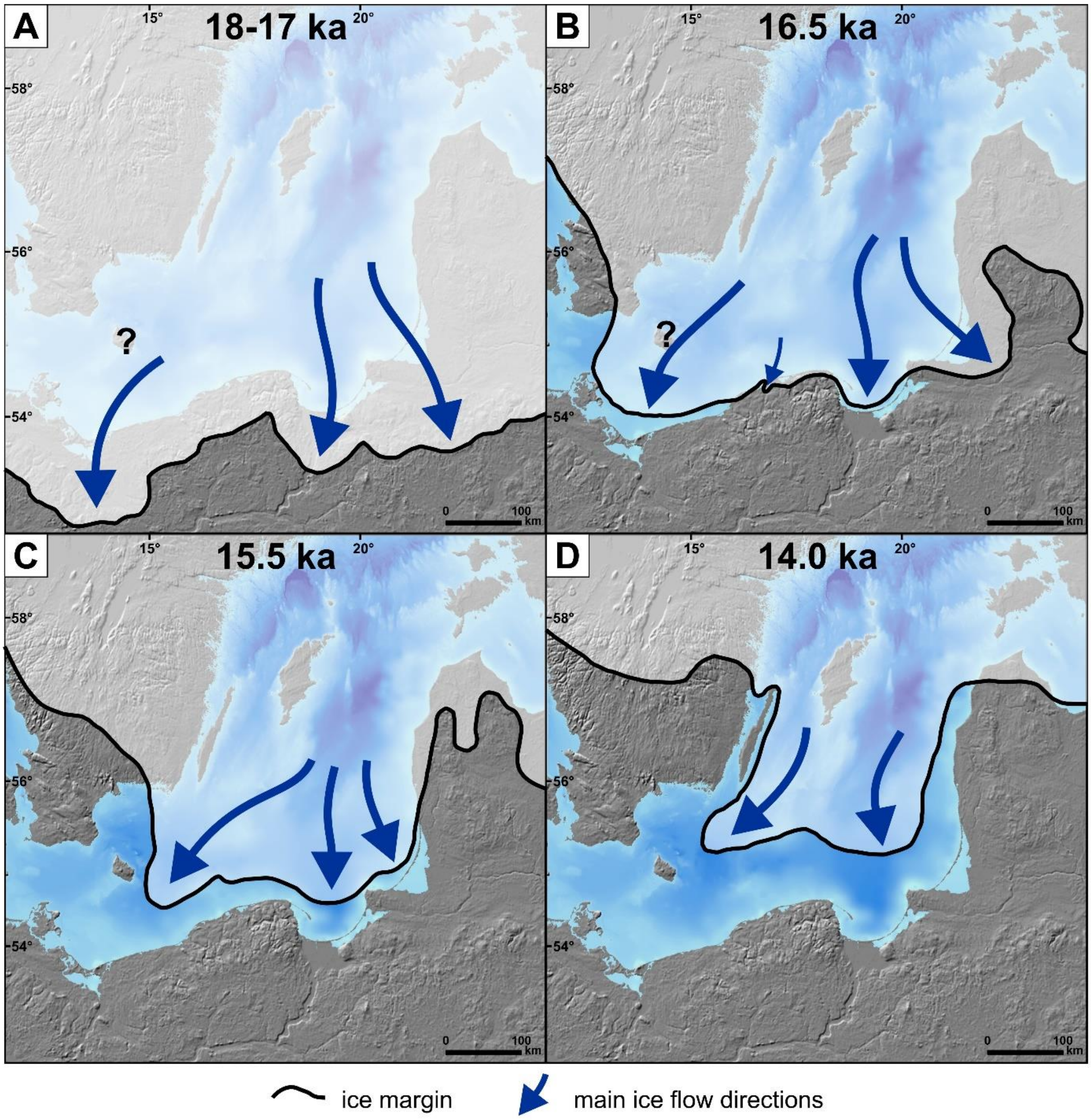

Fig. 7. Time-slice reconstruction for the SIS in the southern Baltic basin and surroundings from the Pomeranian Phase to the Southern Middle Bank Phase. (A) The SIS during the Pomeranian Phase ~18-17 ka. (B) The SIS during the Gardno Phase ~16.5 ka. (C) The SIS during the Słupsk Bank Phase ~15.5 ka. (D) The SIS during the Southern Middle Bank Phase ~14.0 ka. Maps show present distribution of lands (shaded relief of terrain) and sea (blue relief of seafloor).

The age of the two main ice margin stillstands included in our reconstruction is slightly younger that in the model proposed by Stroeven et al. (2016), who calculated deglaciation isochrones that may corresponds to these stillstands at 16 and 15 ka, respectively. Hughes et al. (2016), in their reconstruction of the Eurasian Ice Sheet evolution, also showed that the most probable limit of the southern front of the SIS falls within the time-slices of 16 ka at the Słupsk Bank and 15 ka at the Southern Middle Bank. Our modeling, however, is based on new available geochronological data from the southern Baltic seafloor, which were not included in either of the abovementioned reconstructions of the entire ice sheet. Moreover, the timing of the two main ice margin stillstands during the deglaciation of the southern Baltic basin roughly corresponds to the timing of two cool periods around 15 ka and 14 ka interpreted from paleotemperatures of Greenland based on ice core GISP2 (Alley, 2004). This suggests that the main stillstand phases of the SIS during the last deglaciation of the southern Baltic region were at least partly triggered by climatic fluctuations in the Northern Hemisphere.

7. Conclusions

The Bayesian approach to modeling the chronology of the last deglaciation phases in the southern Baltic basin makes it possible to determine the space-time correlation of ice marginal landforms across the Baltic and to propose a new time-slice reconstruction for this sector of the last SIS. The modeled ages of particular deglaciation phases are 16.5 ± 0.5 ka for the Gardno Phase, 15.6 ± 0.6 ka for the Słupsk Bank Phase, and 13.9 ± 0.5 ka for the Southern Middle Bank Phase. The ice margin limits related to the Gardno Phase, Słupsk Bank Phase, and Southern Middle Bank Phase are correlated to the Halland Coastal moraines and the Middle Lithuanian moraines, the Göteborg moraines and the North Lithuanian (Haanja) moraines, the Vimmerby moraines and the Otepää moraines, respectively. Around 16.5 ka ago, the ice sheet re-advance reached the northernmost parts of the present Baltic coastline in Poland. During the Gardno Phase, the lobate ice margin run possibly from the Halland Coastal moraines on the west, across the northern edges of Rügen, the northern part of the Pomeranian Bay, the moraine arc in the middle Baltic coast of Poland, and the southern edges of the Gdańsk Basin, to the Middle Lithuanian Moraines on the east. Around 15.5 ka, during the Słupsk Bank Phase, the southern Baltic basin was occupied by an extensive ice lobe that spread from the eastern coasts of southern Sweden to the western regions of Lithuania. Similarly, the lobate configuration of the southern front of the SIS occurred about 14.0 ka, when the ice margin retreated slightly to the north and was located on the Southern Middle Bank within the Baltic basin. This ice lobe was probably topographically constrained (by the elongated depression of the Baltic basin), but the main ice streaming corridor of the last SIS, running along the Baltic depression, may also have influenced the configuration of the receding ice margin,

The average retreat rate of the ice margin within the southern Baltic basin was approximately 40–55 m/yr, which is comparable with the retreat rate estimated for deglaciation after the local LGM in northern Poland (~50 m/yr). This suggests that the retreat rate of the ice margin was relatively stable from the early stages of deglaciation after the local LGM to the later stages of the ice sheet recession within the Baltic basin. The margin of the ice sheet there was probably still grounded rather than floating, which may have prevented a more rapid recession and acceleration of the retreat rate in the Baltic basin. The two main ice margin stillstands during deglaciation roughly correspond to the two cool periods around 15 ka and 14 ka interpreted from paleotemperatures of Greenland based on ice core GISP2, which suggests that the last SIS in the southern Baltic responded to climatic fluctuations in the Northern Hemisphere.

The contribution of co-authors to the manuscript is the following:
Karol Tylmann: Conceptualization, Methodology, Validation, Formal analysis, Data Curation, Writing – Original Draft, Visualization.
Szymon Uścinowicz: Conceptualization, Writing – Review & Editing, Supervision.

Declaration of competing interest: The authors declare that they have no known competing financial interests or personal relationships that could have influenced the work reported in this paper.

Acknowledgements: We would like to thank Agnieszka Kubowicz-Grajewska for her valuable help in preparation of Figs. 3 and 7.

Funding: This work was supported by the National Science Center [grant no. 2011/03/B/ST10/05822].

References

Alley, R.B., 2004. GISP2 Ice Core Temperature and Accumulation Data. IGBP PAGES/World Data Center for Paleoclimatology. Data Contribution Series #2004-013. NOAA/NGDC Paleoclimatology Program, Boulder CO, USA.

Andrén, E., Andrén, T., Sohlenius, G., 2000. The Holocene 283 history of the southwestern 284 Baltic Sea as reflected in a sediment core from the Bornholm Basin. Boreas 29: 233–250.

Anjar, J., Larsen, N.K., Håkansson, L., Möller, P., Linge, H., Fabel, D., Xu, S., 2014. A ^{10}Be-based reconstruction of the last deglaciation in southern Sweden. Boreas 43: 132–148.

Borchers, B, Marrero, S, Balco, G., Caffee, M., Goehring, B., Lifton, N., Nishiizumi, K., Phillips, F., Schaefer, J., Stone, J., 2016. Geological calibration of spallation production rates in the CRONUS-Earth project. Quaternary Geochronology 31: 188–198.

Bouvier, V., Johnson, M.D, Påsse, T., 2015. Distribution, genesis and annual-origin of De Geer moraines in Sweden: insights revealed by LiDAR. GFF Journal of the Geological Society of Sweden 137: 319-333.

Bronk Ramsey, C., 2009a. Bayesian analysis of radiocarbon dates. Radiocarbon 51: 337–360.

Bronk Ramsey, C., 2009b. Dealing with outliers and offsets in radiocarbon dating. Radiocarbon 51: 1023–1045.

Bülow, K.V., 1924. Die Diluviallandschaft im nordostlichen Hinterpommern. Jahrbuch d. Preuss. Geologischen Landesanstalt 45: 317–344.

Chiverrell, R.C., Thrasher, I.M., Thomas, G.S.P., Lang, A., Scourse, J.D., van Landeghem, K.J.J., Mccarroll, D., Clark, C.D., O'Cofaigh, C., Evans, D.J.A., Ballantyne, C.K., 2013. Bayesian modelling the retreat of the Irish Sea Ice Stream. Journal of Quaternary Science 28, 200–209.

Cuzzone, J.K., Clark, P.U., Carlson, A.E., Ullman, D.J., Rinterknecht, V.R., Milne, G.A., Lunkka, J-P., Wohlfarth, B., Marcott, S.A., Caffee, M., 2016. Final deglaciation of the Scandinavian Ice Sheet and implications for the Holocene global sea-level budget. Earth and Planetary Science Letters 448: 34–41.

Denton, G.H., Anderson, R.F., Toggweiler, J.R., Edwards, R.L., Schaefer J.M., Putnam A.E., 2010. The Last Glacial Termination. Science 328: 1652–1656.

Dowdeswell, J.A., Batchelor, C.L., Montelli, A., Ottesen, D., Christie, F.D.W., Dowdeswell, E.K., Evans, J., 2020. Delicate seafloor landforms reveal past Antarctic grounding-line retreat of kilometers per year. Science 368: 1020–1024.

Ehlers, J., Gibbard, P. L., Hughes, P. D. (eds.) 2011: Quaternary Glaciations - Extent and Chronology: A Closer Look. Elsevier Amsterdam: 1108 pp.

Galbraith, R.F., Roberts, R.G., Laslett, G.M., Yoshida, H., Olley, J.M., 1999. Optical dating of single and multiple grains of quartz from Jinminum Rock Shelter, Northern 12 Australia. Part I, experimental design and statistical models. Archaeometry 41: 1835–1857.

Fedorowicz, S., Kaszubowski, L., 1982. Wyniki analiz geochemicznych i chronologia radiowęglowa osadów dennych Zalewu Wiślanego. Zeszyty Naukowe Wydziału Biologii i Nauk o Ziemi , Geografia 12: 67–74.

Giedrojć-Juraha, S., 1949. Moreny czołowe okolic jeziora Gardno. Czasopismo Geograficzne 20: 239–244.

Grigoriev, A., Zhamoida, V., Spiridonov, M., Sharapova, A.,Sivkov, V, Ryabchuk, D., 2011. Late-glacial and Holocene palaeoenvironments in the Baltic Sea based on a sedimentary record from the Gdansk Basin. Climate Research 48: 13-21.

Häkansson, S. 1974. University of Lund Radiocarbon Dates VII. Radiocarbon, Vol. 16 F. (3): 307–330.

Hoffmann, G., 2002. Regional geology of the south-western Baltic coast. In: R. Lampe (Ed.) Holocene Evolution of the South-Western Baltic Coast – Geological, Archaeological and Palaeo-environmental Aspects. Greifswalder Geographische Arbeiten, Band 27: 9–12.

Houmark-Nielsen, M., 2008. Testing OSL failures against a regional Weichselian glaciation chronology from southern Scandinavia. Boreas 37: 660–677.

Houmark-Nielsen, M., 2011. Pleistocene Glaciations in Denmark: A closer Look at chronology, Ice Dynamics and Landforms. In: J. Ehlers, P.L. Gibbard, P.D. Hughes (Eds.) Quaternary Glaciations – Extent and Chronology: A Closer Look. Developments in Quaternary Science, 15. Elsevier, Amsterdam: 47–58.

Houmark-Nielsen, M., Linge, H., Fabel, D., Schnabel, C., Xu, S., Wilcken, K.M., Binnie, S., 2012. Cosmogenic surface exposure dating the last deglaciation in Denmark: discrepancies with independent age constraints suggest delayed periglacial landform stabilisation. Quaternary Geochronology 13: 1–17.

Hughes, A.L.C., Gyllencreutz, R., Lohne, Ø.S., Mangerud, J., Inge, J., 2016. The last Eurasian ice sheets – a chronological database and time-slice reconstruction, DATED-1. Boreas 45: 1-45.

Hughes, A.L.C., Winsborrow, M.C.M., Greenwood, S.L., 2021. European Ice Sheet Complex evolution during the Last Glacial Maximum (29–19 ka). In: D. Palacios, P.D. Hughes, J.M. García-Ruiz, N. Andrés (eds.) European Glacial Landscapes. Maximum Extent of Glaciations. Elsevier: 361–372.

Jasiewicz, J., 1999. Glacitektoniczna struktura dupleksu (gardzieńska morena czołowa, klif w Dębinie na zachód od Rowów). In: R.K. Borówka, Z. Młynarczyk, A. Wojciechowski (eds.) Ewolucja geosystemów nadmorskich południowego Bałtyku. Bogucki Wydawnictwo Naukowe, Poznań-Szczecin: 87–93.

Juvigné E., Kozarski, S., Nowaczyk, B., 1995. The occurrence of Laacher See Tephra in Pomerania, NW Poland. Boreas 24: 225–231

Kalm, V., 2006. Pleistocene chronostratigraphy in Estonia, southeastern sector of the Scandinavian glaciation. Quaternary Science Reviews 25: 960–975.

Kopiczyńska-Lamparska, K., 1976. Radiocarbon datings of the Late Glacial and Holocene deposits of western Pomerania. Acta Geologica Polonica 26: 413–418.

Kramarska, R., l991a. Mapa geologiczna dna Bałtyku 1:200000, ark. Ławica Słupska, Ławica Słupska N. Inst. Geol. Warszawa.

Kramarska, R., 1991b. Objaśnienia do mapy geologicznej dna Bałtyku 1:200000, ark. Ławica Słupska, Ławica Słupska N. Państw. Inst. Geol. Warszawa.

Kramarska, R., 1998. Origin and development of the Odra bank in the light of the geologic structure and radiocarbon dating. Geological Quarterly 42: 277–288.

Kramarska, R., Masłowska, M., Michałowska, M., Pikies, R., Śliwiński, Z., Tomczak, A., Uścinowicz, Sz., Zachowicz, J., 1990. Pozycja geologiczna osadów plejstoceńskich z dna Bałtyku Południowego datowanych metodą termoluminescencyjną. Przegląd Geologiczny 38: 248–253.

Lambeck, K., Purcell, A., Zhao, J., Svensson, N.-O., 2010. The Scandinavian Ice Sheet: from MIS 4 to the end of the Last Glacial Maximum. Boreas 19: 410–435.

Lagerlund, L., Persson, K.M., Krzyszkowski, D., Johansson, P., Dobracka, E., Dobracki, R., Panzig, W-A., 1995. Unexpected ice flow directions during the Late Weichselian deglaciation of the south Baltic area indicated by a new lithostratigraphy in NW Poland and NE Germany. Quaternary International 28: 127–144.

Lasberg, K., 2014. Chronology of the Weichselian Glaciation in the southeastern sector of the Scandinavian Ice Sheet. Dissertationes Geologicae Universitatis Tartuensis 37: 1–100.

Lasberg, K., Kalm, V., 2013. Chronology of Late Weichselian glaciation in the western part of the East European Plain. Boreas 42: 995–1007.

Latałowa, M., 1999. Late Vistulian vegetation on Wolin Island (NW Poland) – the preliminary results. Quaternary Studies in Poland, Special Issue: 147–256.

Lundqvist, J., 1986. Late Weichselian glaciation and deglaciation in Scandinavia. Quaternary Science Reviews 5: 269–292.

Lundqvist, J., 1994. The deglaciation. In: National Atlas of Sweden, Geology. Geol. Surv. Sweden: 124–135.

Lundqvist, J., Wohlfarth, B., 2001. Timing and east-west correlation of south Swedish ice marginal lines during the Late Weichselian. Quaternary Science Reviews 20: 1127–1148.

Lüthgens, C., Böse, M., 2011. Chronology of Weichselian main ice marginal positions in north-eastern Germany. E&G Quarternary Science Journal 60: 236–247.

Marks, L., 2002. Last Glacial Maximum in Poland. Quaternary Science Reviews 21: 103–110.

Marks, L., 2005. Pleistocene glacial limits in the territory of Poland. Przegląd Geologiczny 53: 988–993.

Marks, L., 2012. Timing of the Late Vistulian (Weichselian) glacial phases in Poland. Quaternary Science Reviews 44: 81–88.

Marks, L., 2015. Last deglaciation of northern Continental Europe. Cuadernos Investigacion Geografica 41: 279–297.

Marks, L., Dzierżek, J., Janiszewski, R., Kaczorowski, J., Lindner, L., Majecka, A., Makos, M., Szymanek, M., Tołoczko-Pasek, A., Woronko, B., 2016. Quaternary stratigraphy and palaeogeography of Poland. Acta Geologica Polonica 66: 403–427.

Mojski, J.E., 1995. The last Pleistocene ice-sheet and its decay. Pl. XXVI. In: J.E. Mojski et al. (Ed.) Geological atlas of the Southern Baltic, 1 : 500 000. Polish Geological Institute. Sopot-Warszawa.

Mojski, J.E., 2000. The evolution of the southern Baltic coastal zone. Oceanologia 42: 285–303.

Patton, H., Hubbard, A., Andreassen, K., Auriac, A., Whitehouse, P.L., Stroeven, A.P., Shackleton, C., Winsborrow, M., Heyman, J., Hall, A.M., 2017. Deglaciation of the Eurasian ice sheet complex. Quaternary Science Reviews 169: 148–172.

Petelski, K., 1985. Budowa geologiczna moreny czołowej i niecki końcowej lobu gardzieńskiego. Biuletyn Instytutu Geologicznego 348: 89–121.

Pikies, R., 1995. Morphogenesis of Sea Bottom. In: J.E. Mojski (Ed.) Geological atlas of the southern Baltic, 1 : 500 000. Państw. Inst. Geol. Sopot-Warszawa.

Raukas, A., Aboltins, O., Gaigalas, A., 1995. The Baltic States. In: W. Schirmer (Ed.) Quaternary field trip in central Europe. Vol. 1. International Union for Quaternary Research, XIV International Congress. Berlin: 146–151.

Reimer, P.J., Austin, W.E.N., Bard, E., Bayliss, A., Blackwell, P.G., Bronk Ramsey. C,, Butzin, M., Cheng, H., Edwards, R.L., Friedrich, M., Grootes, P.M., Guilderson, T.P., Hajdas, I., Heaton, T.J., Hogg, A.G., Hughen, K.A., Kromer, B., Manning, S.W., Muscheler, R., Palmer, J.G., Pearson, C., van der Plicht, J., Reimer, R.W., Richards, D.A., Scott, E.M., Southon, J.R., Turney, C.S.M., Wacker, L., Adolphi, F., Büntgen, U., Capano, M., Fahrni, S.M., Fogtmann-Schulz, A., Friedrich, R., Köhler, P., Kudsk, S., Miyake, F., Olsen, J., Reinig, F., Sakamoto, M., Sookdeo, A., Talam, S., 2020. The IntCal20 northern hemisphere radiocarbon age calibration curve (0-55 cal ka BP). Radiocarbon 62: 725–757.

Rinterknecht, V.R., Börner, A., Bourlès, D., Braucher, R., 2014. Cosmogenic ^{10}Be age of ice sheet marginal belts in Mecklenburg-Vornpommern, Western Pomerania (northeast Germany). Quaternary Geochronology 19: 42–51.

Rinterknecht, V.R., Clark, P.U., Raisbeck, G.M., Yiou, F., Bitinas, A., Brook, E.J., Marks, L., Zelc, V., Lunkka, J-P., Pavlovskaya, I.E., Piotrowski, J.A., Raukas, A., 2006. The last deglaciation of the southeastern sector of the Scandinavian Ice Sheet. Science 311: 1449–1452.

Rotnicki, K., Borówka, K., 1995. The last cold period in the Gardno-Łeba Coastal Plain. Journal of Coastal Research. Special Issue No. 22: 225–229.

Saarse, L., Heinsalu, A., Veski, S., 2012. Deglaciation chronology of the Pandivere and Palivere ice-marginal zones in Estonia. Geological Quarterly 56: 353–362.

Sinclair, S.N., Licciardi, J.M., Campbell, S.W., Madore, B.M., 2018. Character and origin of De Geer moraines in the seacoast region of New Hampshire, USA. Journal of Quaternary Science 33: 225–237.

Stroeven, A.P., Hättestrand, C., Kleman, J., Heyman, J., Fabel, D., Fredin, O., Goodfellow, B.W., Harbor, J.M., Jansen, J.D., Olsen, L., Caffee, M.W., Fink, D., Lundqvist, J., Rosqvist, G.C., Strömberg, B., Jansson, K.N., 2016. Deglaciation of Fennoscandia. Quaternary Science Reviews 147: 91–121.

Stroeven, A.P., Heyman, J., Derek, F., Björck, S., Caffee, M.W., Fredin, O., Harbor, J.M., 2015. A new Scandinavian reference ^{10}Be production rate. Quaternary Geochronology 29: 104–115.

Uścinowicz, Sz., 1995. The evolution of the southern Baltic during the Late Glacial and the Holocene. Plate XXVII. in: J.E. Mojski (Ed.) Geological atlas of the Southern Baltic, 1 : 500 000. Państw. Inst. Geol. Sopot-Warszawa.

Uścinowicz, Sz., 1996. Deglacjacja obszaru południowego Bałtyku (Deglaciation of the southern Baltic area), (in Polish with English summary). Biuletyn Państwowego Instytutu Geologicznego 373: 177-193.

Uścinowicz, Sz., 1999. Southern Baltic area during the last deglaciation. Geological Quarterly 43: 137–148.

Uścinowicz, Sz., 2010. De Geer moraines on the Słupsk Bank. The 10th International Marine Geological Conference. The Baltic Sea geology. VSEGEI St. Petersburg, Russia. Abstracts volume: 139–141.

Uścinowicz, Sz., 2014. Baltic Sea Continental Shelf. in: F. Chiocci, A. Chivas (ed.) Continental Shelves of the World, Their Evolution During Last Glacio-Eustatic Cycle. Geological Society Memoir No.41, London: 69–89.

Uścinowicz, Sz., Zachowicz, J., 1991. Geological map of the Baltic Sea bottom, 1:200000, sheet Łeba-Słupsk. Państw. Inst. Geol. Warszawa.

Uścinowicz, Sz., Adamiec, G., Bluszcz, A., Jegliński, W., Jurys, L., Miotk-Szpiganowicz, G., Moska, P., Pączek, U., Piotrowska, P., Poręba, G., Przezdziecki, P., Uścinowicz, G., 2019. Chronology of the last ice sheet decay on the southern Baltic area based on dating of glaciofluvial and ice-dammed lake deposits. Geological Quarterly 63: 192–207.

Witkowski. A., ,Witak, M., 1993. Budowa geologiczna dna Zatoki. In: K. Korzeniewski (Ed.) Zatoka Pucka. Instytut Oceanografii Uniwersytetu Gdańskiego, Gdańsk: 309-315.

Woldstedt, P., 1925. Die grosser Endmoränenzüge Norddeutschland. Zeitschrift der Deutschen Geologischen Gesellschaft 77: 172–184.

Woldstedt, P., 1935. Über die Geschichte des Küstriner Beckens und der Eberswalder Pforte. Jahrbuch der Königlichen Preussischen Geologischen Landesanstalt 56: 274–291.

Wysota, W., Molewski, P., Sokołowski, R.J., 2009. Record of Vistula ice lobe advance in the Late Weichselian glacial sequence in north-central Poland. Quaternary International 207: 26–41.

Tylmann, K., Rinterknecht, V.R., Woźniak, P.P., Bourlès, D., Schimmelpfennig, I., Guillou, V., ASTER Team, 2019. The Local Last Glacial Maximum of the southern Scandinavian Ice Sheet front: Cosmogenic nuclide dating of erratics in northern Poland. Quaternary Science Reviews 219: 36–46.

Zachowicz, J., 1995. Quaternary geological profiles (II). Pl. XVIII. In: J. E. Mojski et al. Ed..) Geological atlas of the Southern Baltic, 1:500000. Państw. Inst. Geol. Sopot - Warszawa.

Zachowicz. J., Uścinowicz. Sz.. 1997. Późnoplejstoceńskie i holoceńskie osady z obszaru Zalewu Wiślanego. In: W. Florek (Ed.) Geologia i geomorfologia środkowego pobrzeża i południowego Bałtyku 3. Wyższa Szkoła Pedagogiczna w Słupsku: 29–37.

Suplementary Materials

Tab. S1. Radiocarbon dates of sediments overlying till of the last glaciation in the southern Baltic region. The conventional ^{14}C ages were calibrated according to *IntCal20* calibration curve (Reimer et al., 2020)

Site/core	Coordinates		^{14}C age [ka BP]	^{14}C calibrated age [ka b2k]	Laboratory code	Material dated	Locality	References
	φ	λ						
R-86	54°05.00’	14°38.00’	12.01 ± 0.10	13.95 ± 0.12	Gd-10048	peat	Pomeranian Bay	Kramarska (1998)
W-4	54°15.70’	14°44.20’	14.06 ± 0.22	17.15 ± 0.33	Gd-2928	peat	Pomeranian Bay	Kramarska (1998)
VR 072-2	54°08.61’	15°00.04’	12.21 ± 0.06	14.21 ± 0.15	Poz-43787	peat	Pomeranian Bay	Polish Geological Institute - National Research Institute archive
V 32-4	54°14.31’	14°34.44’	12.25 ± 0.06	14.29 ± 0.18	Poz-43797	peat	Pomeranian Bay	Polish Geological Institute - National Research Institute archive
V 40-3	54°00.74’	14°34.58’	11.91 ± 0.05	13.82 ± 0.11	Poz-43799	peat	Pomeranian Bay	Polish Geological Institute - National Research Institute archive
Niechorze Eo4	54°05.58’	15°29.00’	12.92 ± 0.33	15.45 ± 0.55	Gd-373	peat	western Polish coast	Kopiczyńska-Lamparska (1976)
Warnowo	53°57.56’	14°36.00’	12.01 ± 0.12	13.95 ± 0.16	Gd-2524	gyttja	Wolin	Latałowa (1992)
Warnowo	53°55.99’	14°33.89’	11.68 ± 0.13	13.61 ± 0.14	Gd-10052	peat	Wolin	Juvigne et al. (1995)
11K02/A	55°02.21’	15°44.00’	8.80 ± 0.15	9.92 ± 0.20	Gd-6317	marine mud	Bornholm Basin	Zachowicz (1995)
21163-13	55°22.65’	15°23.85’	9.91 ± 0.12	11.48 ± 0.19	Ua-13504	clay	Bornholm Basin	Andren et al. (2000)
R10 (192)	55°34.70’	17°25.90’	10.22 ± 0.10	12.00 ± 0.25	Gd-10304	peat	Southern Middle Bank	Polish Geological Institute - National Research Institute archive
14 097B	54°55.66’	17°08.52’	10.51 ± 0.07	12.53 ± 0.16	Gd-4187	peat	Słupsk Bank	Uścinowicz, Zachowicz (1991)
GT5A/82	55°21.95’	18°46.56’	8.62 ± 0.20	9.75 ± 0.27	Gd-9174	marine mud	Gotland Basin	Zachowicz (1995)
303700-7	54°49.34’	19°11.01’	11.80 ± 0.50	14.04 ± 0.68	RGI-531	clay	Gdańsk Basin	Grigorjev et al. (2011)
IIIa	54°23.40’	19°41.70’	11.24 ± 0.11	13.20 ± 0.11	Gd-773	limnic mud	Vistula Lagoon	Fedorowicz, Kaszubowski (1982)
ZW3	54°20.80’	19°16.70’	12.27 ± 0.20	14.46 ± 0.36	Gd-10246	peat	Vistula Lagoon	Zachowicz, Uścinowicz (1997)
4/2001	54°31.08’	18°41.35’	12.20 ± 0.06	14.19 ± 0.14	Poz-485	gyttja	Gulf of Gdańsk	Polish Geological Institute - National Research Institute archive
W2	54°39.25’	18°31.60’	11.92 ± 0.08	13.85 ± 0.13	Gd-7744	gyttja	Puck Lagoon	Polish Geological Institute - National Research Institute archive
ZP18A	54°40.20’	18°30.10’	11.30 ± 0.16	13.25 ± 0.15	Gd-4838	gyttja	Puck Lagoon	Witkowski, Witak (1993)
Szary Dwór	54°48.07’	18°09.02’	12.42 ± 0.28	14.68 ± 0.45	Gd-4261	silt	Eastern Polish coast	Polish Geological Institute - National Research Institute archive
Łeba Barrier 35	54°40.60’	17°14.00’	13.80 ± 0.27	16.77 ± 0.39	Gd-6117	peat	central Polish coast	Rotnicki, Borówka (1995)
Łeba Barrier 101	54°40.60’	17°05.00’	14.30 ± 0.15	17.50 ± 0.24	Gd-4776	clay	central Polish coast	Rotnicki, Borówka (1995)
Orzechowo	54°35.08’	16°54.02’	11.80 ± 0.12	13.73 ± 0.14	Lu-763	peat remnants	central Polish coast	Häkansson (1974)

Tab. S2. Luminescence dates significant for the timing of the last SIS retreat in the southern Baltic region.

Site/core	Coordinates φ	Coordinates λ	Age [ka]	Laboratory code	Material dated	Method	Locality	Landform	References
460	55°33.51'	17°20.76'	13.20 ± 2.00	UG-793	sand	TL	Southern Middle Bank	glaciofluvial delta	Kramarska et al. (1990)
S1-1	54°59.02'	17°06.03'	11.05 ± 0.84	GdTL-2023	sand	OSL	Słupsk Bank	glaciofluvial delta	Uścinowicz et al. (2019)
			9.77 ± 0.83	GdTL-2024	sand	OSL	Słupsk Bank	glaciofluvial delta	
			12.16 ± 0.94	GdTL-2025	sand	OSL	Słupsk Bank	glaciofluvial delta	
S1-2	54°59.36'	17°06.00'	11.45 ± 0.84	GdTL-2030	sand	OSL	Słupsk Bank	glaciofluvial delta	
			11.11 ± 0.97	GdTL-2031	sand	OSL	Słupsk Bank	glaciofluvial delta	
			10.06 ± 0.76	GdTL-2032	sand	OSL	Słupsk Bank	glaciofluvial delta	
S2-1	54°54.99'	16°40.64'	11.33 ± 0.91	GdTL-2062	sand	OSL	Słupsk Bank	glaciofluvial delta	
			12.10 ± 0.83	GdTL-2063	sand	OSL	Słupsk Bank	glaciofluvial delta	
S2-2	54°55.37'	16°38.74'	16.60 ± 1.40	GdTL-2068	sand	OSL	Słupsk Bank	glaciofluvial delta	
			21.30 ± 2.00	GdTL-2069	sand	OSL	Słupsk Bank	glaciofluvial delta	
			15.60 ± 1.20	GdTL-2070	sand	OSL	Słupsk Bank	glaciofluvial delta	
			14.30 ± 1.20	GdTL-2071	sand	OSL	Słupsk Bank	glaciofluvial delta	
ZA-1	54°52.57'	17°08.29'	41.10 ± 3.00	GdTL-2034	silty sand	OSL	south of Słupsk Bank	ice-marginal lake plain	
			47.20 ± 2.90	GdTL-2035	silty sand	OSL	south of Słupsk Bank	ice-marginal lake plain	
			76.30 ± 5.40	GdTL-2036	silty sand	OSL	south of Słupsk Bank	ice-marginal lake plain	
			37.10 ± 2.40	GdTL-2037	silty sand	OSL	south of Słupsk Bank	ice-marginal lake plain	
			70.50 ± 5.00	GdTL-2038	silty sand	OSL	south of Słupsk Bank	ice-marginal lake plain	
ZA-2	54°51.91'	16°58.90'	135.00 ± 12.00	GdTL-2079	silty sand	OSL	south of Słupsk Bank	ice-marginal lake plain	
			59.90 ± 4.40	GdTL-2080	silty sand	OSL	south of Słupsk Bank	ice-marginal lake plain	
			14.60 ± 1.40	GdTL-2081	silty sand	OSL	south of Słupsk Bank	ice-marginal lake plain	
			12.92 ± 0.64	GdTL-2082	silty sand	OSL	south of Słupsk Bank	ice-marginal lake plain	
			14.51 ± 0.81	GdTL-2083	silty sand	OSL	south of Słupsk Bank	ice-marginal lake plain	
ZA-3	54°51.40'	17°32.91'	11.09 ± 0.79	GdTL-2048	silty sand	OSL	south-west of Stilo Bank	ice-marginal lake plain	
Żelazo 1	54°39.56'	17°16.50'	15.38 ± 1.00	GdTL-2164	sand	OSL	Gardno-Łeba Lowland	coastal ridge	
			13.73 ± 0.84	GdTL-2165	sand	OSL	Gardno-Łeba Lowland	coastal ridge	
Żelazo 2	54°39.64'	17°15.80'	15.56 ± 0.98	GdTL-2166	sand	OSL	Gardno-Łeba Lowland	coastal ridge	
			16.70 ± 1.10	GdTL-2167	sand	OSL	Gardno-Łeba Lowland	coastal ridge	
Łokciowe	54°41.28'	17°16.37'	14.72 ± 0.92	GdTL-2168	sand	OSL	Gardno-Łeba Lowland	coastal ridge	
			14.05 ± 0.79	GdTL-2169	sand	OSL	Gardno-Łeba Lowland	coastal ridge	
Nowęcin 1	54°45.29'	17°35.80'	12.35 ± 0.80	GdTL-2170	sand	OSL	Gardno-Łeba Lowland	coastal ridge	
			15.42 ± 0.90	GdTL-2171	sand	OSL	Gardno-Łeba Lowland	coastal ridge	
Nowęcin 2	54°45.30'	17°35.88'	11.03 ± 0.73	GdTL-2172	sand	OSL	Gardno-Łeba Lowland	coastal ridge	
			16.13 ± 0.94	GdTL-2173	sand	OSL	Gardno-Łeba Lowland	coastal ridge	

Tab. S3. OxCal code of the initial model for the deglaciation chronology.

```
Options()
 {
  BCAD = FALSE;
  kIterations = 100;
  PlusMinus = FALSE;
  SD1 = FALSE;
  SD2 = TRUE;
  SD3 = FALSE;
 };
 Plot()
 {
  Outlier_Model("BALTIC",T(5),U(0,4),"t");
  Sequence("BALTICretreat")
  {
   Boundary("START");
   After(Age("POM_Phase", 17000, 1000));
   Boundary("Gardno Phase");
   Phase("post-Gardno")
   {
    C_Date("Gd-4776", 17500, 238)
    {
     Outlier(0.05);
    };
    C_Date("Gd-6117", 16774, 388)
    {
     Outlier(0.05);
    };
   };
   Boundary("Slupsk Bank Phase");
   Phase("Slupsk Bank")
   {
    C_Date("GdTL-2025", 12160, 940)
    {
     Outlier(0.05);
    };
    C_Date("GdTL-2024", 9770, 830)
    {
     Outlier(0.05);
    };
    C_Date("GdTL-2023", 11050, 840)
    {
     Outlier(0.05);
    };
    C_Date("GdTL-2032", 10060, 760)
    {
     Outlier(0.05);
    };
    C_Date("GdTL-2031", 11110, 970)
    {
     Outlier(0.05);
    };
    C_Date("GdTL-2030", 11450, 840)
    {
     Outlier(0.05);
    };
    C_Date("GdTL-2063", 12100, 830)
    {
     Outlier(0.05);
    };
    C_Date("GdTL-2062", 11330, 910)
    {
     Outlier(0.05);
    };
    C_Date("GdTL-2071", 14300, 1200)
    {
     Outlier(0.05);
    };
    C_Date("GdTL-2070", 15600, 1200)
    {
     Outlier(0.05);
    };
    C_Date("GdTL-2069", 21300, 2000)
    {
     Outlier(0.05);
    };
C_Date("GdTL-2068", 16600, 1400)
    {
     Outlier(0.05);
    };
    C_Date("GdTL-2083", 14510, 810)
    {
     Outlier(0.05);
    };
    C_Date("GdTL-2082", 12920, 640)
    {
     Outlier(0.05);
    };
    C_Date("GdTL-2081", 14600, 1400)
    {
     Outlier(0.05);
    };
    C_Date("GdTL-2048", 11090, 790)
    {
     Outlier(0.05);
    };
    C_Date("GdTL-2164", 15380, 1000)
    {
     Outlier(0.05);
    };
    C_Date("GdTL-2165", 13730, 840)
    {
     Outlier(0.05);
    };
    C_Date("GdTL-2166", 15560, 980)
    {
     Outlier(0.05);
    };
    C_Date("GdTL-2167", 16700, 1100)
    {
     Outlier(0.05);
    };
    C_Date("GdTL-2168", 14720, 920)
    {
     Outlier(0.05);
    };
    C_Date("GdTL-2169", 14050, 790)
    {
     Outlier(0.05);
    };
    C_Date("GdTL-2170", 12350, 800)
    {
     Outlier(0.05);
    };
    C_Date("GdTL-2171", 15420, 900)
    {
     Outlier(0.05);
    };
    C_Date("GdTL-2172", 11030, 730)
    {
     Outlier(0.05);
    };
    C_Date("GdTL-2173", 16130, 940)
    {
     Outlier(0.05);
    };
   };
   Boundary("Southern Middle Bank Phase");
   Phase("Southern Middle Bank")
   {
    C_Date("UG-793", 13200, 2000)
    {
     Outlier(0.05);
    };
   };
   Before(Age("Gotland", 13000, 700));
   Boundary("END");
  };
 };
```